ETHIOPIAN INTERNATIONAL JOURNAL OF MULTIDISCIPLINARY RESEARCH

eISSN: 2349-5715 pISSN: 2349-5707

Volume: 12, Issue 04, April-2025 SJIF 2019: 4.702 2020: 4.737 2021: 5.071 2022: 4.919 2023: 6.980 2024: 7,662

THE IMPACT OF HEAT TREATMENT ON THE STRUCTURAL AND SPECTRAL CHARACTERISTICS OF THE RAMAN SPECTRUM OF MONOCRYSTALLINE SILICON

S.Z.Zaynabidonov, B.M. Ergashev,

Sh.Odilov, J.S.Madaminjonov

Andijan state university named after Z.M. Babur, Andijan, Uzbekistan

Abstract: This study investigates how thermal treatment affects the structural characteristics of monocrystalline silicon. Analyzing the Raman spectra of n-type and p-type silicon samples reveals low-intensity peaks with broad half-widths, indicating interactions of transverse optical phonons. This suggests the presence of small crystalline regions and amorphous zones within the samples. At a temperature of 1000°C, silicon and oxygen atoms begin to rearrange, facilitating the formation of amorphous clusters. This transformation is particularly noticeable in p-type silicon samples, where thermal treatment leads to the emergence of nanocrystallites. However, as the temperature rises to 1100°C, these nanocrystallites are converted back into amorphous clusters due to the presence of impurity atoms. This phenomenon clearly demonstrates that elevated temperatures can significantly impact the atomic structure of silicon, altering both its crystalline and amorphous regions. The changes in these regions result in substantial modifications to the overall structural properties of silicon. These observations highlight the intricate relationship between temperature and atomic behavior in shaping material characteristics. Understanding this complex interplay is essential for grasping the effects of thermal treatments on semiconductor materials, particularly silicon. Such insights are crucial for optimizing semiconductor manufacturing processes and ensuring the desired performance characteristics of final products.

Keywords: Monocrystalline silicon, thermal treatment, Raman spectroscopy, optical phonons, amorphous clusters, nanocrystals.

INTRODUCTION

Monocrystalline silicon is a foundational material in modern electronics, highly valued for its precise structural, physical, and electrical properties, all of which require meticulous control. These properties can be deliberately modified through a variety of processing techniques, among which thermal treatment plays a particularly crucial role. Thermal processing of monocrystalline silicon serves as an essential method for manipulating its crystalline structure at the atomic scale, leading to significant enhancements or deliberate alterations in its mechanical, electrical, and optical characteristics [1].

The primary objectives of heat treatment include the reduction of structural defects, the improvement of mechanical strength, and the achievement of a more uniform atomic distribution during doping processes. The degree of structural transformation induced by thermal treatment is highly dependent on both the temperature and the duration of the exposure, as different thermal regimes yield distinct modifications in the silicon's microstructure and associated properties. High-temperature treatments can, for instance, facilitate the annihilation of dislocations and vacancies, while lower-temperature processes may be used to finely tune dopant diffusion and activation.

eISSN: 2349-5715 pISSN: 2349-5707

Volume: 12, Issue 04, April-2025 SJIF 2019: 4.702 2020: 4.737 2021: 5.071 2022: 4.919 2023: 6.980 2024: 7,662

Given its critical role, understanding the effects of thermal processing on the crystalline structure of monocrystalline silicon is essential for optimizing its performance in advanced technological applications. This article provides a comprehensive examination of how various thermal treatment conditions influence the atomic arrangement, defect dynamics, and resultant physical properties of monocrystalline silicon, offering insights into the underlying mechanisms that govern these transformations.

MATERIALS AND METHODS

In this research, monocrystalline silicon wafers with n-type and p-type conductivity were selected as the primary material. These wafers, which were produced using the Czochralski method, exhibited specific resistivities of 5 and 20 Ω·cm, respectively. One notable drawback of monocrystalline silicon generated via the Czochralski method is the elevated concentration of background oxygen and carbon atoms within the crystals. The oxygen and carbon concentrations can reach approximately 2×10^{18} cm^{-3} and 5×10^{16} cm^{-3}, respectively. The ongoing challenge in crystal growth technology remains the presence of oxygen atoms in silicon, which continues to be a critical issue.

RESULTS AND DISCUSSION

Figure 1 presents the Raman spectrum of the initial n-type silicon (n-Si) sample. The spectrum reveals that the most intense peak is located at 526.1 cm^{-1}. This peak corresponds to the activation of first-order longitudinal optical (LO) phonons within the silicon crystal lattice, which is indicative of a high degree of structural integrity and crystallinity. Previous studies [2,3] have consistently reported that the most prominent Raman peak for silicon typically appears around 520 cm^{-1}. In the present study, however, the observed peak is shifted to a higher frequency (526.1 cm^{-1}), suggesting the presence of internal mechanical stresses within the silicon crystal lattice. These stresses are likely introduced during crystal growth or through subsequent mechanical and chemical processing of the control samples.

An evaluation of the sample crystallinity can also be performed by comparing the intensity of the primary Raman peak with the average level of the inelastic background signal. According to established criteria, a ratio of approximately 103 signifies high crystallinity, a ratio of 102 indicates above-average crystallinity, and a ratio of 10 is associated with low crystallinity. For the sample under investigation, this ratio is measured to be 30, which corresponds to a medium to low level of crystallinity. This finding supports the notion that mechanical stresses, as well as local distortions induced by mechanical and chemical treatments, have influenced the crystalline quality. Moreover, variations in the ordering of oxygen, carbon, and phosphorus atoms—elements that also contribute to the electronic conductivity of silicon—may additionally impact the observed crystallinity.

The full width at half maximum (FWHM) of the main Raman peak was determined to be approximately 10.8 cm^{-1}. In an ideal, defect-free silicon crystal lattice, the FWHM typically ranges between 3 and 5 cm^{-1} [4]. The significantly broader FWHM observed here, nearly double the typical value, further supports the hypothesis of mechanical stress and defect formation within the crystal lattice. The Raman spectrum begins with a signal increase at 67.2 cm^{-1}, with most peaks occurring against a relatively high inelastic background level (lower than 102) (see Figure 1a). This elevated background may be attributed to the interaction of acoustic phonons, the presence of dislocations or other defects within the silicon microstructure, as well as background impurities [5]. High background levels can also arise from the presence of clusters, microcracks, or amorphous components embedded within the crystalline matrix. A broad, low-intensity peak observed at 154.4 cm^{-1} does not correspond

eISSN: 2349-5715 pISSN: 2349-5707

Volume: 12, Issue 04, April-2025 SJIF 2019: 4.702 2020: 4.737 2021: 5.071 2022: 4.919 2023: 6.980 2024: 7,662

to primary phonon modes but is rather attributed to second-order phonon processes. This feature may be linked to various types of defects in the silicon crystal lattice, including impurity atoms such as phosphorus, boron, or other elements. Additionally, the thermal history of the sample—including processes such as growth, thermal annealing, and quenching—may influence the emergence of these second-order features [6].

Further features of interest include a peak at 303.0 cm^{-1}, commonly associated with the interaction (combination or difference) of second-order transverse acoustic (TA) and transverse optical (TO) phonons. This peak can also be linked to the presence of amorphous phases or microcrystalline inclusions in the silicon matrix, reflecting particular structural characteristics and dynamic behavior of the material.

Moreover, a peak at 462.3 cm^{-1} is observed, attributed to the interaction of second-order transversely activated phonons. Additionally, a weak but distinct peak at 657.5 cm^{-1} is present, resulting from the combination of two second-order longitudinal optical phonons, leading to an energy summation effect. Together, these spectral features provide critical insights into the complex phonon interactions within the crystal lattice, highlighting the intricate nature of structural and electronic dynamics in the n-Si samples under study [7].

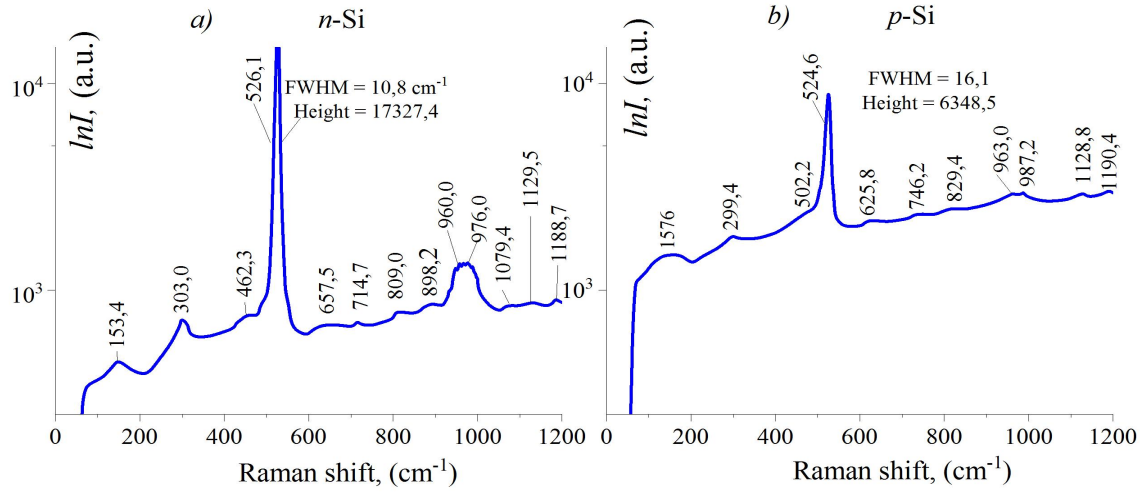

Figure 1. Raman spectra of n-Si and p-Si samples.

In the Raman spectrum of the initial n-type silicon (n-Si) sample, high-frequency peaks were detected at 714.7 cm^{-1}, 809.0 cm^{-1}, and 898.2 cm^{-1}. These peaks are likely the result of third-order interactions, involving combinations of longitudinal and transverse optical phonons, arising from the summation of the energies of three third-order phonons [8]. The presence of these peaks may reflect the existence of impurity states within the silicon, as well as insights into the internal structure and phonon dynamics, highlighting the complexity of interactions within the crystal lattice. Additionally, high-frequency peaks at 960.0 cm^{-1} and 976.0 cm^{-1} were observed, both characterized by broad full widths at half

eISSN: 2349-5715 pISSN: 2349-5707

Volume: 12, Issue 04, April-2025 SJIF 2019: 4.702 2020: 4.737 2021: 5.071 2022: 4.919 2023: 6.980 2024: 7,662

maximum (FWHM). These features likely originate from generalized peaks resulting from the summation of energies from third-order longitudinal optical phonons. Their presence suggests the formation of various nanocrystalline structures within the silicon matrix, attributed to the combination of silicon and oxygen atoms. The interaction between silicon and oxygen atoms, in various structural modifications, plays a significant role in the formation of crystallites and clusters [9]. Moreover, high-frequency peaks were observed at 1079.4 cm^{-1}, 1129.5 cm^{-1}, and 1188.7 cm^{-1}, resulting from the combination of three longitudinal optical phonons. These peaks deviate from the standard phonon modes of pristine silicon, providing deeper insights into the interactions and structural changes occurring at the microstructural level. Such findings are crucial for understanding the fundamental behavior of silicon, particularly in the context of its application in advanced electronic and optoelectronic technologies. Figure 2a shows the Raman spectrum of the control n-Si sample after thermal treatment at 1000 °C for 2 hours. When compared with the initial n-Si spectrum (Figure 1a), noticeable differences are evident. The main peak, corresponding to the activation of primary longitudinal optical phonons in silicon, is slightly shifted to a lower frequency at 525.7 cm^{-1}. Furthermore, the intensity of this peak decreased by approximately 50%, while the FWHM remained relatively unchanged at around 10.8 cm^{-1}. The ratio of the main peak's intensity to the average inelastic background was found to be approximately 88, indicating a moderate reduction in crystallinity due to the heat treatment.

The overall inelastic background level in the Raman spectrum of the control n-Si sample after thermal processing at 1000 °C showed significant reductions: a 28% decrease at low frequencies and an almost 90% decrease at high frequencies. These spectral modifications likely result from the redistribution of background impurities such as oxygen and carbon, as well as phosphorus atoms contributing to electronic conductivity [10]. The thermal-induced reordering of these atomic species is believed to relieve internal mechanical stresses, thereby enhancing the structural quality of the silicon lattice. The Raman spectrum of the n-Si sample after thermal treatment also exhibits a broad phonon mode beginning at 63.7 cm^{-1}, with a notably wide FWHM of approximately 298.0 cm^{-1}. This suggests the formation of phonon modes associated with the partial ordering of defect structures within the lattice due to thermal effects. Additional low-intensity peaks with broad FWHM, arising from interactions of second- and third-order transverse-activated phonons, are more pronounced in the spectrum post-treatment. These features imply that the heat treatment promotes the growth of nanocrystallites formed through the interaction of silicon atoms with oxygen, alongside their crystallographic reorganization. Such microstructural changes are expected to influence the material's mechanical, optical, and electronic properties, a factor of considerable importance for optimizing semiconductor device performance.

Figure 2b presents the Raman spectrum of the n-Si sample after thermal treatment at 1100 °C for 2 hours. This spectrum reveals substantial changes compared to both the initial Raman spectrum (Figure 1a) and the spectrum following treatment at 1000 °C. The main LO phonon activation peak exhibits a partial shift towards a higher frequency at 526.1 cm^{-1}. The peak's intensity has decreased by a factor of approximately 1.6 compared to the sample treated at 1000 °C, and by a factor of about 1.3 relative to the original n-Si sample. Interestingly, the FWHM of this peak is reduced to around 9.7 cm^{-1}, representing a narrowing of 0.4 cm^{-1} compared to previous measurements, which suggests a reduction in the defect density or an improvement in lattice uniformity. Moreover, the ratio of the intensity of the main peak to the average inelastic background increased significantly to approximately 193, indicative of enhanced structural order. The background levels in the spectrum show further reductions: approximately 56% for low-frequency scattering and nearly 92% for high-frequency scattering. These

eISSN: 2349-5715 pISSN: 2349-5707

Volume: 12, Issue 04, April-2025 SJIF 2019: 4.702 2020: 4.737 2021: 5.071 2022: 4.919 2023: 6.980 2024: 7,662

findings confirm that thermal treatment at higher temperatures facilitates substantial rearrangement of oxygen and carbon impurities, as well as phosphorus dopants, thereby relieving mechanical stresses and improving the structural and electronic quality of the silicon material.

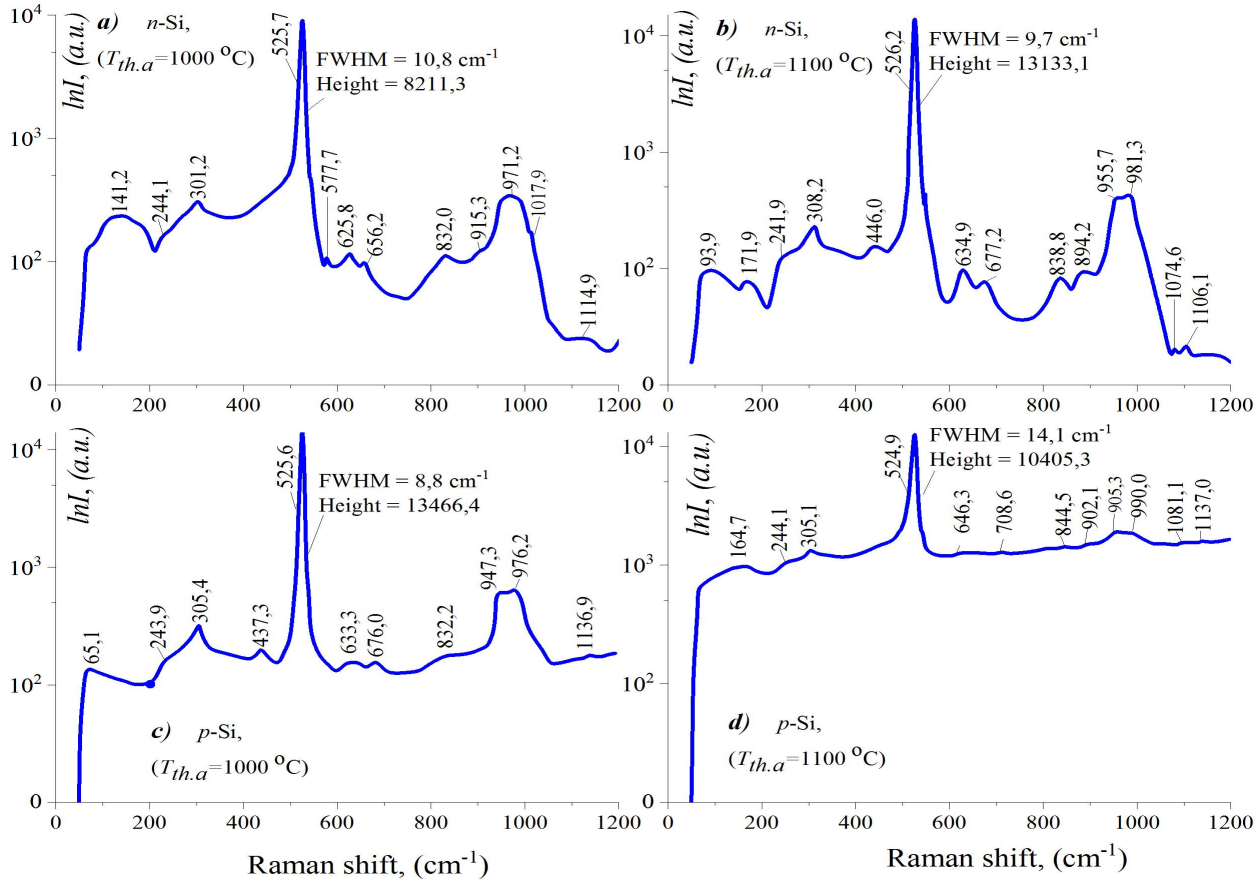

Figure 2. Raman spectra of control samples n-Si and p-Si after thermal treatment at temperatures of 1000 °C and 1100 °C.

Additionally, splits in the peaks, resulting from the interactions of second- and third-order transverse optical phonons, are observed. The intensity of these peaks increases, while their FWHM decreases. This suggests an increase in the size of nanocrystallites, which form due to the merging of clusters that exhibit amorphous properties at smaller scales throughout the entire volume. These clusters incorporate both silicon and oxygen atoms as a result of thermal processing.

Figure 2-c illustrates the Raman spectrum of the p-Si sample after thermal treatment at 1000 °C for 2 hours. This spectrum demonstrates significant differences compared to the original Raman spectrum of the p-Si sample (Figure 1-b). Notably, the primary peak related to the activation of LO phonons has shifted to higher frequencies (~ 1 cm^{-1}) and appears at 525.6 cm^{-1}. Additionally, the intensity of this peak has increased by 1.6 times, while its full width at half maximum (FWHM) has decreased by approximately half to ~ 8.8 cm^{-1}. It was also found that the ratio of the intensity of this peak to the average inelastic background is 108. The overall inelastic background has decreased, with low-frequency scattering reduced by 78% and high-frequency scattering reduced by approximately 86%. Furthermore, the spectrum begins with a peak at 63.7 cm^{-1} and shows that nearly all peaks, resulting from the interactions of second- and third-order transverse optical phonons, appear at a lower level of

eISSN: 2349-5715 pISSN: 2349-5707

Volume: 12, Issue 04, April-2025 SJIF 2019: 4.702 2020: 4.737 2021: 5.071 2022: 4.919 2023: 6.980 2024: 7,662

inelastic background compared to the original Raman spectrum of the p-Si sample and are clearly visible. The observed changes in the Raman spectrum of the p-Si sample after thermal treatment at 1000 °C suggest alterations in the size and crystallographic organization of nanocrystallites formed due to the interaction between silicon and oxygen atoms.

Figure 2-d presents the Raman spectrum of the control p-Si sample after thermal treatment at 1100 °C for 2 hours. This spectrum shows notable changes compared to the Raman spectra of the original p-Si sample (Figure 1-b). Specifically, the main peak associated with the activation of LO phonons has shifted to higher frequencies by 0.3 cm^{-1} compared to the peak in the original p-Si spectrum and to lower frequencies by 0.3 cm^{-1} compared to the peak in the spectrum of the p-Si sample treated at 1000 °C. It is observed at 524.9 cm^{-1}. Furthermore, the intensity of this peak has decreased by 1.6 times compared to the peak in the original p-Si spectrum and by 1.3 times compared to the peak after treatment at 1000 °C. The FWHM of this peak is approximately 14.1 cm^{-1}, which is 1.1 times smaller than in the original p-Si spectrum and 1.6 times larger than after treatment at 1000 °C. It was also found that the ratio of the intensity of this peak to the average inelastic background is 8.8. The overall inelastic background has also decreased by 14-17% at low, medium, and high scattering frequencies compared to the original Raman spectrum of the p-Si sample, while it increased by 67% compared to the spectrum of the p-Si sample after thermal treatment at 1000 °C. Additionally, the peaks resulting from the interactions of second- and third-order transverse optical phonons in the p-Si sample after treatment at 1000 °C appear with uncertain and weak intensity. This suggests that during thermal treatment at 1100 °C, there is a redistribution and bonding of silicon and oxygen atoms, forming small amorphous clusters that impart amorphous properties to the material.

CONCLUSION

This study comprehensively examined the effects of thermal treatment on the crystalline structure and phonon dynamics of n-type and p-type monocrystalline silicon (n-Si and p-Si) samples through Raman spectroscopy. The results demonstrate that thermal processing at 1000 °C and 1100 °C induces significant structural modifications, which are reflected in the shifts, intensities, and full widths at half maximum (FWHM) of the primary and secondary Raman peaks. For the n-Si samples, thermal treatment at 1000 °C led to a moderate decrease in the intensity of the main longitudinal optical (LO) phonon peak and a slight shift to lower frequencies, accompanied by a reduction in the inelastic background, indicating partial defect reordering and impurity redistribution. Further treatment at 1100 °C resulted in a slight shift of the LO phonon peak to higher frequencies, a notable increase in the peak-to-background ratio, and a narrowing of the FWHM, suggesting enhanced lattice ordering, reduced mechanical stresses, and improved crystalline quality. The observed third-order phonon interactions and broadening of high-frequency peaks highlight the formation of nanocrystallites and complex silicon-oxygen bonding processes induced by thermal effects. In the case of p-Si samples, thermal treatment at 1000 °C improved crystallinity, as evidenced by the narrowing of the main phonon peak, a significant increase in its intensity, and a marked reduction in the background signal. However, treatment at 1100 °C resulted in a decrease in peak intensity and a partial broadening of the FWHM, alongside the reappearance of a higher background level. These changes indicate the formation of amorphous clusters due to the redistribution of silicon and oxygen atoms, leading to a partial degradation of the crystalline structure at higher treatment temperatures.

Overall, the findings confirm that thermal treatment is a powerful method for tailoring the structural and electronic properties of monocrystalline silicon by modulating defect densities, impurity distributions, and nanocrystallite formation. The optimal thermal conditions depend on the desired

eISSN: 2349-5715 pISSN: 2349-5707

Volume: 12, Issue 04, April-2025 SJIF 2019: 4.702 2020: 4.737 2021: 5.071 2022: 4.919 2023: 6.980 2024: 7,662

balance between crystallinity enhancement and the prevention of amorphous phase development. These insights are crucial for improving the material quality of silicon used in high-performance semiconductor and optoelectronic applications.In the Raman spectra of n-Si and p-Si samples, low-intensity peaks with broad full width at half maximum (FWHM) are observed. These peaks arise due to the interactions of second- and third-order transverse optical phonons. They manifest on surfaces and in defect regions as a result of the combination of silicon and oxygen atoms in various configurations, leading to the formation of small fragments with both crystalline and amorphous properties. During thermal treatment of n-Si samples at 1000 °C, reconfiguration of silicon and oxygen atoms occurs, resulting in increased size and crystallographic alignment of amorphous clusters. At 1100 °C, these clusters merge, forming nanocrystals. Similarly, during the thermal treatment of p-Si samples at 1000 °C, silicon and oxygen atoms combine to form nanocrystals, which grow in size and become crystallographically organized. However, at 1100 °C, due to the redistribution and merging of background impurity atoms, small amorphous clusters are formed.

REFERENCES:

1. A.I. Prostomolotov, Yu.B. Vasiliev, and A.N. Petlitsky, “Mechanics of defect formation during growth and heat treatment of singlecrystal silicon,” **4**, 1716–1718 (2011). http://www.unn.ru/pages/e-library/vestnik/19931778_2011_-_4-4_unicode/147.pdf
2. R.T.-P. Lee, K.-M. Tan, T.-Y. Liow, C.-S. Ho, S. Tripathy, G.S. Samudra, D.-Z. Chi, and Y.-C. Yeo, “Probing the ErSi1.7 Phase Formation by Micro-Raman Spectroscopy,” Journal of The Electrochemical Society, **154**(5) H361-H364 (2007). https://doi.org/10.1149/1.2710201
3. D. Casimir, H. Alghamdi, I.Y. Ahmed, R. Garcia-Sanchez, and P. Misra, “Raman Spectroscopy of Graphene, Graphite and Graphene Nanoplatelets,” in: 2D Materials, edited by C. Wongchoosuk, and Y. Seekaew, (IntechOpen, 2019). https://doi.org/10.5772/intechopen.84527
4. K. Adu, M. Williams, M. Reber, R. Jayasingha, H.R. Gutierrez, and G. Sumanasekera, “Probing Phonons in Nonpolar Semiconducting Nanowires with Raman Spectroscopy,” J. Nanotechnol. **2**, 264198 (2012). https://doi.org/10.1155/2012/264198
5. K. Ali, S. Khan, M. Zubir, and M.Z.M. Jafri, “Spin-on doping (SOD) and diffusion temperature effect on re-combinations/ideality factor for solar cell applications,” Chalcogenide Letters, **9**, 457–463 (2012). https://www.chalcogen.ro/457_KhuramAli.pdf
6. M.A. Lourenço, Z. Mustafa, W. Luduczak, L. Wong, R.M. Gwilliam, and K.P. Homewood, “High temperature dependence Dy3+ in crystalline silicon in the optical communication and eye-safe spectral regions,” Optics Letters, **38**(18), 3669-3672 (2013). https://doi.org/10.1364/OL.38.003669
7. M. Li, Y. Liu, Y. Zhang, X. Han, T. Zhang, Y. Zuo, C. Xie, et al., “Effect of the Annealing Atmosphere on Crystal Phase and Thermoelectric Properties of Copper Sulfide,” ACS Nano, **15**(3), 4967-4978 (2021). https://doi.org/10.1021/acsnano.0c09866
8. I.L. Shulpina, R.N. Kyutt, V.V. Ratnikov, I.A. Prokhorov, I.Zh. Bezbakh, M.P. Shcheglov, “Methods of X-ray diffraction diagnostics of heavily doped semiconductor single crystals,” Journal of Technical Physics, **80**(4), 105 (2010). https://journals.ioffe.ru/articles/viewPDF/9970
9. V. Mankad, S. Gupta, P. Jha, N. Ovsyuk, and G. Kachurin, “Low-frequency Raman scattering from Si/Ge nanocrystals in different matrixes caused by acoustic phonon quantization,” J. Appl. Phys. **112**, 54318 (2012). https://doi.org/10.1063/1.4747933
10. M.O. Atajonov, Q. Mamarasulov, at all. “Research of solar panel model based on photovoltaic module,” In AIP Conference Proceedings, **I**(1), 3244 (2024). https://doi.org/10.1063/5.0241785